Title

GABAB receptor allosteric modulators exhibit pathway-dependent and species-selective activity

Journal

Pharmacology Research & Perspectives, 5(2)

ISSN

2052-1707

Authors

Sturchler, Emmanuel
Li, Xia
Ladino, Maria Lourdes
et al.

Publication Date

2017-04-01

DOI

10.1002/prp2.288

Peer reviewed

PRP Pharmacology Research & Perspectives
Open Access

ORIGINAL ARTICLE

$GABA_B$ receptor allosteric modulators exhibit pathway-dependent and species-selective activity

Emmanuel Sturchler[1,§], Xia Li[2,§], Maria de Lourdes Ladino[1,a], Kasia Kaczanowska[3,b], Michael Cameron[1], Patrick R. Griffin[1], M. G. Finn[3,c], Athina Markou[2] & Patricia McDonald[1]

[1]Department of Molecular Therapeutics, The Scripps Research Institute, 130 Scripps way, Jupiter, Florida 33458
[2]Department of Psychiatry, University of California San Diego, 9500 Gilman Drive, La Jolla, California 92093
[3]Department of Chemistry, The Scripps Research Institute, 10550 North Torrey Pines Road, La Jolla, California 92037

Keywords
Allosteric modulator, biased signaling, functional selectivity, $GABA_B$ receptor, ortholog selectivity

Correspondence
Patricia McDonald, Department of Molecular Therapeutics, The Scripps Research Institute, 130 Scripps Way, Florida Jupiter, FL 33458.
Tel: +1-561-228-2222; Fax: 561-228-3081;
E-mail: mcdonaph@scripps.edu
and
Athina Markou, Department of Psychiatry, M/C 0603, School of Medicine, University of California San Diego, 9500 Gilman Drive, La Jolla, CA 92093-0603;
Tel: +1-858-534-1572;
Fax: +1-858-534-9917;
E-mail: amarkou@ucsd.edu

Present addresses
[a]School of Medicine, Vanderbilt University, 2215 Garland Ave, Nashville, Tennessee, 37232
[b]Department of Chemistry, University of California, San Diego, 9500 Gilman Drive, La Jolla, California, 92093
[c]Georgia Institute of Technology, School of Chemistry and Biochemistry, 901 Atlantic Drive, Atlanta, Georgia 30332

Funding Information
This work was supported by National Institutes of Health grant U19 DA026838.

Received: 21 June 2016; Revised: 2 November 2016; Accepted: 30 November 2016

Pharma Res Per, 5(2), 2017, e00288, doi:10.1002/prp2.288

doi: 10.1002/prp2.288

[§]These authors contributed equally to this work.

Abstract

Positive modulation of the $GABA_B$ receptor ($GABA_BR$) represents a potentially useful therapeutic approach for the treatment of nicotine addiction. The positive allosteric modulators (PAMs) of $GABA_BR$ GS39783 and BHF177 enhance GABA-stimulated [^{35}S]GTPγS-binding, and have shown efficacy in a rodent nicotine self-administration procedure reflecting aspects of nicotine dependence. Interestingly, the structural related analog, NVP998, had no effect on nicotine self-administration in rats despite demonstrating similar pharmacokinetic properties. Extensive in vitro characterization of GS39783, BHF177, and NVP998 activity on $GABA_BR$-regulated signaling events, including modulation of cAMP, intracellular calcium levels, and ERK activation, revealed that these structurally related molecules display distinct pathway-specific signaling activities that correlate with the dissimilarities observed in rodent models and may be predictive of in vivo efficacy. Furthermore, these $GABA_BR$ allosteric modulators exhibit species-dependent activity. Collectively, these data will be useful in guiding the development of $GABA_BR$ allosteric modulators that display optimal in vivo efficacy in a preclinical model of nicotine dependence, and will identify those that have the potential to lead to novel antismoking therapies.

Abbreviations

cAMP, cyclic adenosine monophosphate; CHO cells, Chinese hamster ovary cells; CRC, concentration–response curve; ERK, Extracellular signal-regulated kinases; GABA, γ-aminobutyric acid; GPCR, G protein-coupled receptor; HEK293 cells, human embryonic kidney 293 cells; PAM, Positive allosteric modulator.

Introduction

The $GABA_BR$ is an obligate heterodimer, where heterodimerization between the $GABA_BR1$ and $GABA_BR2$ subunits form the functional $GABA_BR$. The $GABA_BR1$ subunit contains the γ-aminobutyric acid (GABA) orthosteric agonist binding site, whereas the $GABA_BR2$ subunit couples to heterotrimeric $G_{i/0}$ proteins. Agonism of the $GABA_BR$ leads to a decrease in cAMP levels via inhibition of adenylyl cyclase, increased intracellular calcium (New et al. 2006), and phosphorylation of the extracellular-signal regulated protein kinase 1/2 ($ERK_{1/2}$) (Tu et al. 2007) (Vanhoose et al. 2002). Thus, $GABA_BR$ couples to several distinct intracellular signal transduction pathways. Dysfunction of $GABA_BR$ signaling is associated with various disorders including epilepsy, anxiety, depression, sleep disorders, cognitive impairment, and drug addiction (Pinard et al. 2010). Hence, $GABA_BR$ agonists, such as baclofen, are of potential utility in the management of such diseases. However, side effects, principally sedation, tolerance, and motor impairment, limit their therapeutic use.

Emerging concepts in receptor pharmacology, such as functional selectivity and allosteric modulation, have attracted considerable interest recently from a therapeutic perspective. Functional selectivity or ligand-bias refers to the ability of a particular ligand to activate one signaling pathway to the exclusion of others suggesting that one can fine-tune the signaling output of a target receptor. Allosteric modulation arises from molecules that bind to a site on the receptor that is topographically distinct from the orthosteric binding site of the receptor's natural ligand (Christopoulos 2002). Allosteric ligands modulate not only orthosteric ligand efficacy but can also display intrinsic activity. The discovery of positive allosteric modulators (PAMs) of the $GABA_BR$, was first reported by Urwyler et al. (2001). CGP7930 was found to specifically act on the $GABA_BR2$ subunit, yet it exhibited intrinsic agonist activity suggesting allosteric communication between subunits (Binet et al. 2004). In preclinical studies, CGP7930 in combination with baclofen has shown improved therapeutic-like benefits over baclofen alone with respect to sedation (Carai et al. 2004), depression-like (Mombereau et al. 2004), and drug-seeking behaviors in rodents (Lhuillier et al. 2007; Mombereau et al. 2007). High throughput screening of small molecule libraries led to the identification of the positive allosteric modulator N'-dicyclopentyl-2-methylsulfanyl-5-nitro-pyrimidin-4,6-diamine (GS39783) (Urwyler et al. 2003, 2005; Guery et al. 2007). This chemical scaffold was led to the development of analogs BHF177 and NVP998 which have been demonstrated to enhance GABA-dependent $GABA_BR$ activation (Guery et al. 2007). Subsequently, it was shown that BHF177 was effective at decreasing nicotine self-administration, supporting the potential utility of $GABA_BR$ PAMs as novel pharmacotherapies for nicotine addiction. It should be noted here that nicotine is the main psychoactive ingredient in tobacco that is believed to perpetuate the harmful tobacco smoking. Interestingly, it was found that GS39783 could only achieve comparable in vivo efficacy as BHF177 when co-administered with a subeffective dose of the $GABA_BR$ agonist CGP44532 (Paterson et al. 2008).

Here, we show that the structurally related GS39783/BHF177 analog NVP998 failed to decrease nicotine self-administration in the rat despite having similar in vivo pharmacokinetic properties. To test whether the dissimilarities observed in vivo could be explained by differences in the in vitro pharmacological activity profile of these allosteric modulators, we developed a multiple cell-based functional assay platform to investigate the effects of GS39783, BHF177, and NVP998 on $GABA_BR$-mediated cellular responses including cAMP production, intracellular Ca^{2+} mobilization, and $ERK_{1/2}$ phosphorylation. The modulation of $GABA_BR$-mediated cellular responses was investigated using both rat and human $GABA_BR$-expressing cellular systems. Collectively, our results reveal the existence of functional selectivity and species-selective modulation of $GABA_BR$ signaling by these structurally related $GABA_BR$ allosteric modulators.

Materials and methods

Intravenous nicotine self-administration

Animals

Male Wistar rats (Charles River, Raleigh, NC), weighing 300–350 g at the beginning of the experiments, were housed two per cage in an environmentally controlled vivarium on a reversed 12 h/12 h light/dark cycle throughout the experiment. All behavioral testing occurred during the dark phase of the light/dark cycle. Rats had ad libitum access to food and water initially and were subsequently put on a food-restricted diet of 20 g rat chow per day during behavioral training and testing. All procedures were conducted in accordance with the guidelines from the National Institutes of Health and the Association for the Assessment and Accreditation of Laboratory Animal Care and were approved by the Institutional Animal Care and Use Committees of our institutions.

Apparatus

Standard operant conditioning chambers (24 × 30 × 28 cm; Med Associates, St. Albans, VT) were used in all experiments as described previously (Liechti et al. 2007a).

Food self-administration under a fixed-ratio schedule of reinforcement

Naive rats were gradually trained to lever press for food (45 mg Noyes food pellets) on a fixed-ratio five timeout 20 sec (FR5 TO20 s) schedule during 1 h sessions for 3 weeks (5 days per week). After successful acquisition of stable food self-administration, NVP998 (0, 20, 40 and 80 mg/kg, p.o.; 1 h pretreatment) was administered using a within-subjects Latin-square design. At least 7 days elapsed between drug administrations, and rats were required to exhibit stable baseline performance prior to drug administration.

Nicotine self-administration under a fixed-ratio schedule of reinforcement

Naive rats were gradually trained to lever press for food on an FR5 TO20 s schedule over a period of 5–7 days. After food training, all the rats were surgically prepared with an intravenous catheter inserted into the right jugular vein under isoflurane (1–3% in oxygen) anesthesia as described previously (Liechti and Markou 2007b). For the rats used for the assessment of intracerebroventricular (i.c.v.) administration of NVP998 on nicotine self-administration, guide cannulae (26 gage; Plastics One, Roanoke, VA) were implanted bilaterally 1 mm above the cerebroventricular (from bregma: anterior/posterior, 0.9 mm; medial/lateral, ±1.8 mm; dorsal/ventral, −3.4 mm from dura; angle: 10 degree) using a stereotaxic frame (David Kopf Instruments, Tujunga, CA). After surgery, the animals were allowed to recover for at least 5 days before nicotine self-administration training was initiated. During nicotine self-administration training, animals self-administered nicotine (0.03 mg/kg/infusion) on an FR5 TO20 s schedule during 1 h sessions for 4–5 weeks (5 days per week). After successful acquisition of stable nicotine self-administration, NVP998 (0, 20, 40, and 80 mg/kg, p.o.; 1 h pretreatment) was administered using a within-subjects Latin-square design. At least 7 days elapsed between drug administrations, and rats were required to exhibit stable baseline performance prior to drug administration. For the rats that were prepared with intracranial guide cannulae, NVP998 (0, 4 and 8 μg/side, 0.5 h pretreatment) was administered using a between-subjects design.

Nicotine self-administration under a progressive-ratio schedule of reinforcement

The food training, intravenous catheterization surgery, and nicotine self-administration training under the fixed-ratio schedule were the same as that described in section 2.7.4. After successful acquisition of stable nicotine self-administration under fixed-ratio, rats were switched to the progressive-ratio schedule of reinforcement as described previously (Paterson et al. 2008). In this schedule, the level press numbers for a single nicotine infusion were progressively increased. The breakpoint was defined as the highest ratio completed before the first 1 h period during which no injections were earned. The number of responses required to earn a nicotine infusion on the progressive ratio was determined by the exponential progression $[5e^{(0.25 \times (\text{infusion number} + 3)} - 5]$, with the first two values replaced by 5 and 10 (modified from (Richardson and Roberts 1996)), so that the response requirements for successive reinforcers were 5, 10, 17, 24, 32, 42, 56, 73, 95, 124, 161, 208, etc. The effects of NVP998 (0, 20, 40 and 80 mg/kg, p.o.; 1 h pretreatment) were assessed in animals that showed stable nicotine self-administration behavior using a within-subjects Latin-square design.

Pharmacokinetic procedures

To assure that differences in the self-administration tests were not due to pharmacokinetics or CNS exposure, rats were administered 20 mg/kg GS39783, BHF177, or NVP998 by oral gavage and plasma levels were quantitated at 0.5, 1, and 1.5 h. These times represented the beginning, middle, and end of the self-administration experiments where compound was administrated 30 min prior to initiating the testing session. Brains were collected at the 1.5 h time point. Plasma was generated by standard centrifugation techniques and immediately frozen. Plasma and brain were mixed with acetonitrile (1:5 v:v or 1:5 w:v, respectively). Plasma samples were vortexed and allowed to sit on ice for 15 min, and brain samples were disrupted with a probe tip sonicator. Samples are centrifuged through a Millipore Multiscreen Solvinter 0.45 micron low binding PTFE hydrophilic filter plate and drug levels were determined using an ABSciex 5500 mass spectrometer (Framingham, MA, U.S.A.) with multiple reaction monitoring and mass transitions of 338.2→202.1 for GS39783, 348.2→254.2 for BHF177, and 359.2→265.2 for NVP998. Brain concentrations were quantitated as drug per mg tissue and converted to a molar concentration by assuming a conversion of 1 g tissue equals 1 mL.

Compounds

GABA, baclofen, CGP54626, and GS39783 were purchased from Tocris Biosciences (Avonmouth, Bristol, United Kingdom). BHF177 and NVP998 were synthesized and provided by Dr. M.G. Finn, Georgia Tech, GA. (−) Nicotine hydrogen tartrate (Sigma, St. Louis, MO) was dissolved in saline (0.9%) and pH-adjusted to 7.4 (±0.5) with 1 mol/L sodium hydroxide solution. Nicotine doses are reported as freebase concentrations.

Cell culture

A stable CHO (Chinese hamster ovary) cell line expressing a functional $GABA_BR$ comprised of human $GABA_BR1b$ and rat $GABA_BR2$ (CHO_{RGBR}; a kind gift from Dr. K. Kaupmann, Novartis, Basel, Switzerland), a stable CHO cell line expressing a functional $GABA_BR$ comprised of human $GABA_BR1b$ and human $GABA_BR2$ (CHO_{HGBR}) and a stable HEK293 (human embryonic kidney) cell line expressing a functional $GABA_BR$ comprised of human $GABA_BR1b$ and human $GABA_BR2$ (HEK_{HGBR}) were used for all cell-based experiments described herein. CHO_{RGBR}, CHO_{HGBR}, and HEK_{HGBR} cells were cultured in F12 medium and DMEM, respectively, supplemented with 10% fetal bovine serum, 1 mg/mL geneticin, and 250 μg/mL zeocin.

Measurement of cAMP levels

CHO_{RGBR} and HEK_{HGBR} cells were seeded into white-walled 384-well plates at a density of 2000 and 2500 cells per well, respectively, in 20 μL of growth media and cultured overnight at 37°C, 5% CO_2. The following day medium was removed and replaced with 20 μL of Hanks' balanced salt solution (HBSS), 20 mmol\L HEPES, pH 7.4. After 1 h incubation at room temperature (RT), 5 μL of induction medium (HBSS, 20 mmol\L HEPES containing forskolin; 50 μmol/L and 150 μmol/L for CHO_{RGBR} and HEK_{HGBR}, respectively) (MP biochemical, Irvine, CA 92618 USA), and the test compounds together with GABA were added to the cells at the indicated concentrations. After 10 min and 20 min incubations at RT for the CHO_{RGBR} and the HEK_{HGBR} cells, respectively, cAMP levels were measured using Cisbio' (Bedford, MA 01730 USA) cAMP dynamic HTRF assay kit as per the manufacturer's instructions. Briefly, induction medium was removed and the cells were lysed in 10 μL of 1:1 PBS-lysis buffer containing cAMP labeled with the acceptor dye d2. Subsequently, 10 μL of 1:1 PBS-lysis buffer containing cAMP-specific antibody labeled with cryptate was added to each well. After 1 h at room temperature, the amount of cAMP in lysate samples was quantified according to the manufacturer's instructions using the Envision plate reader (PerkinElmer, Shelton, CT 06484-4794 USA). Concentration–response curves (CRC) were recorded with four wells per concentration and experiment. The effects of the compounds were calculated relative to the stimulation obtained with a maximally active concentration of GABA. CRCs were determined by nonlinear regression analysis using Prism software (GraphPad Software Inc., San Diego, CA).

Measurement of intracellular calcium concentration

CHO_{RGBR} and HEK_{HGBR} cells were seeded into black-walled 384-well plates at a density of 10,000 and 20,000 cells per well, respectively, in 20 μL of growth media and cultured overnight at 37°C, 5% CO_2. The following day the medium was removed and replaced with 20 μL of loading medium consisting of HBSS, 20 mmol/L HEPES, 2.5 mmol/L probenicid, and fluorescent indicator Fluo-4 AM (Invitrogen, Carlsbad, CA 92008 USA). After 1 h incubation, cell and compound plates were placed into the fluorescence imaging plate reader (FLIPR; Molecular Devices, Sunnyvale, CA 94089 USA). Compounds (prepared as 5× solution in HBSS and 20 mmol/L HEPES, pH 7.4) were added at time = 10 sec and changes in fluorescence were monitored over a period of 250 sec following excitation at a wavelength of 488 nm and detection at 510–560 nm. Relative changes over baseline ($\Delta F/F$) were determined. Concentration–response curves were recorded with four wells per concentration and experiment. The effects of compounds were calculated relative to the stimulation obtained with a maximally active concentration of GABA. CRCs were determined by nonlinear regression analysis using Prism software (GraphPad Software Inc., San Diego, CA).

In cell $ERK_{1/2}$ phosphorylation Western blot

To determine the time point at which maximum $ERK_{1/2}$ phosphorylation occurs after $GABA_BR$ activation, CHO_{RGBR} and HEK_{HGBR} cells were seeded at 5000 cells/well in a 384-well plate and incubated overnight at 37°C, 5% CO_2. The next day the medium was removed and replaced with 20 μL of HBSS, 20 mmol/L HEPES. After 1 h incubation at 37°C, 5% CO_2, 5 μL of HBSS 20 mmol/L HEPES containing GABA was added to the plate and incubated at room temperature for the indicated time periods. After incubation, the medium was discarded and the cells were fixed in 4% paraformaldehyde in PBS for 20 min. Cells were then washed 3× with PBS. After discarding the last wash, cells were permeabilized for 20 min with 0.2% Triton X-100 in PBS then washed 3× in PBS. After discarding the last wash, Odyssey blocking buffer was added and the plate was rocked for 1 h at room temperature. Odyssey blocking buffer was then removed, and rabbit anti-phospho-ERK (1/150 in Odyssey blocking buffer) and mouse

anti-ERK (1/200 in Odyssey blocking buffer) were added to the plate and incubated overnight at 4°C. The following day the plates were washed three times with 0.1% Tween 20 in PBS. Infrared probe-labeled goat-anti-mouse and anti-rabbit (1/200 in 0.025% Tween 20 in PBS) were added. The plates were incubated for 1 h at room temperature, washed with 0.025% Tween 20, and scanned by the Odyssey infrared scanner. Data were acquired using the scanner software, and analyzed using Prism software (GraphPad Software Inc., San Diego, CA).

Measurement of $ERK_{1/2}$ phosphorylation

CHO_{RGBR} and HEK_{HGBR} cells were seeded at 4000 cells/well in a 384-well plate and incubated overnight at 37°C, 5% CO_2. The following day medium was removed and replaced with 20 μL of HBSS, 20 mmol/L HEPES, pH 7.4. After 1 h incubation, 5 μL of HBSS, 20 mmol/L HEPES containing GABA in the presence or absence of test compounds was added to the wells and incubated at room temperature for 5 min. After incubation, the medium was discarded and the cells were lysed in 16 *M*l lysis buffer provided in the Cellul'erk HTRF cell-based assay (Cisbio). After 10 min of incubation, 4 μL of detection buffer containing the HTRF conjugates was added in each well. After 2 h at room temperature, the amount of phospho-ERK in the lysate samples was quantified according to the manufacturer's instruction using the Envision plate reader (PerkinElmer). Concentration–response curves were recorded with four wells per concentration and experiment. The effects of compounds were calculated relative to the stimulation obtained with a maximally active concentration of GABA. CRCs were determined by nonlinear regression analysis using Prism software (GraphPad Software Inc., San Diego, CA).

Measurement of Cellular Impedance

Impedance measurements were performed using the CellKey system (Molecular Devices). CHO_{RGBR} cells were seeded at a density of 30,000 cells/well into CellKey microplates (MDS SCIEX) in 100 μL of growth medium and cultured overnight. The following day, cells were washed three times with assay buffer (HBSS containing 20 mmol/L HEPES, pH 7.4) and allowed to equilibrate for 30 min. After a 90 sec read to establish a baseline, ligands (5× in assay buffer) were added online in the CellKey instrument and the changes of cellular impedance were measured over 10 min. For the desensitization assay, cells were incubated with GABA or the PAMs for 20 min. Subsequently, the cells were washed three times with assay buffer to remove the ligand and allowed to equilibrate in assay buffer for 30 min before being stimulated a second time with a fixed concentration of GABA at an EC90 (5× in assay buffer). The changes of cellular impedance induced by a second addition were measured over 10 min. The effects of GABA and the PAMs were calculated relative to the stimulation obtained with a maximally active concentration of GABA. CRCs were determined by nonlinear regression analysis using Prism software (GraphPad Software Inc., San Diego, CA).

Results

Effects of NVP998 on nicotine self-administration

The plasma concentrations of GS39783, BHF177, and NVP998, in rats treated with 20 mg/kg of each of the three compounds were 482 ± 83 ng/mL (1.4 ± 0.2 μmol/L), 125 ± 3 ng/mL (0.4 ± 0.008 μmol/L), and 407 ± 210 ng/mL (1.1 ± 0.6 μmol/L) at the beginning of the experiment (concentration at 1 h) and 472 ± 16 ng/mL (1.4 ± 0.04 μmol/L), 145 ± 13 ng/mL (0.4 ± 0.03 μmol/L), and 284 ± 176 ng/mL (0.8 ± 0.5 μmol/L) after testing (concentration at 2 h), respectively (Table 1). The corresponding brain concentrations of GS39783, BHF177, and NVP998, were 635 ± 114 ng/mL (1.9 μmol/L), 979 ± 80 ng/mL (2.8 μmol/L), and 321 ± 147 ng/mL (0.9 μmol/L), respectively, (Table 1). These data indicate that the $GABA_B$R allosteric ligands displayed low micromolar plasma and brain concentration during testing. However, in contrast to BHF177

Table 1. Plasma and brain concentrations of NVP998, BHF177, and GS39783, before and at the end of the experiment in rat.

			Plasma exposure						Brain exposure	
			Conc. 0.5 h		Conc. 1 h		Conc. 2 h		Conc. 2 h	
Drug	Route	Dose (mg/kg^{-1})	ng/mL	μmol/L	ng/mL	μmol/L	ng/mL μmol/L	μmol/L	ng/mL μmol/L	μmol/L
GS39783	p.o.	20	500 ± 67	1.5 ± 0.2	482 ± 83	1.4 ± 0.2	472 ± 16	1.4 ± 0.04	635 ± 114	1.9 ± 0.3
BHF177	p.o.	20	76 ± 44	0.2 ± 0.1	125 ± 3	0.4 ± 0.008	145 ± 13	0.4 ± 0.03	979 ± 80	2.8 ± 0.2
NVP998	p.o.	20	425 ± 184	1.2 ± 0.5	407 ± 210	1.1 ± 0.6	284 ± 176	0.8 ± 0.5	321 ± 147	0.9 ± 0.4

(20 mg/kg p.o) that significantly decreased nicotine self-administration in rats (Paterson et al. 2008), systemic administration of NVP998 (20, 40 and 80 mg/kg, p.o.) did not affect nicotine self-administration under a fixed-ratio or a progressive-ratio schedule of reinforcement (Fig. 1A and B). The lack of effects of systemic NVP998 on nicotine self-administration might be due to poor brain exposure because this compound had the lowest brain concentration among these three PAMs. However, this possibility was excluded because i.c.v. administration of NVP998 also had no effect on nicotine self-administration (Fig. 1C). Thus, we hypothesized that the differences in drug responsiveness may result from differences in the intrinsic properties of the compound that are not observed using traditional GTPγS-binding assays. Therefore, we further investigated the effect of the allosteric ligands on $GABA_B$R-mediated, changes in intracellular cAMP levels, intracellular $[Ca^{2+}]$, and $ERK_{1/2}$ phosphorylation.

Effects of GS39783 and analogs on $GABA_B$R-mediated inhibition of cAMP production

Upon GABA binding, $GABA_B$R preferentially couples to the $G\alpha_i$ pathway, inhibiting adenylyl cyclase activity, and thus decreasing the level of intracellular cAMP. Therefore, we first determined the effects of GS39783, BHF177, and NVP998 on GABA-mediated inhibition of forskolin (FSK)-stimulated cAMP production using a CHO cell line expressing a functional $GABA_B$R comprised of human $GABA_B$R1b and rat $GABA_B$R2 (CHO_{RGBR}), or stable HEK293 and CHO cell lines expressing a functional $GABA_B$R comprised of human $GABA_B$R1b and human $GABA_B$R2 (HEK_{HGBR} and CHO_{HGBR}, respectively). As expected, the addition of GABA resulted in a concentration-dependent inhibition of FSK-stimulated cAMP production with an EC_{50} value of 0.67 μmol/L, 0.52 μmol/L, and 0.99 μmol/L in CHO_{RGBR}, HEK_{HGBR}, and CHO_{HGBR} cells, respectively (Figs. 2–4). The inhibition of cAMP

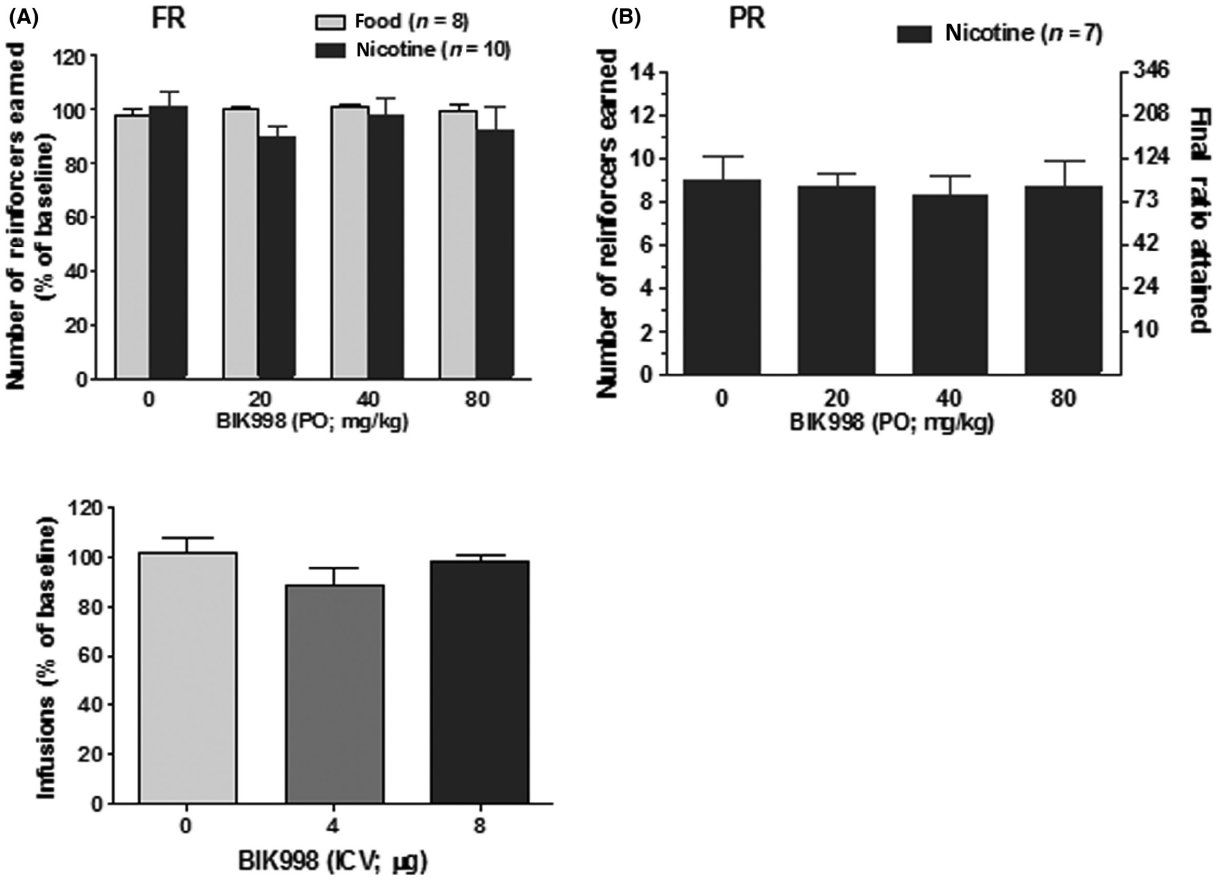

Figure 1. Effects of the $GABA_B$R-positive allosteric modulator NVP998, on nicotine self-administration in rats. Systemic administration of NVP998 (20, 40 and 80 mg/kg) had no effect on nicotine or food self-administration under fixed- or progressive-ratio schedules of reinforcement in rats. Similar lack of effect was also observed after i.c.v. administration of NVP998 (4 and 8 μg/side).

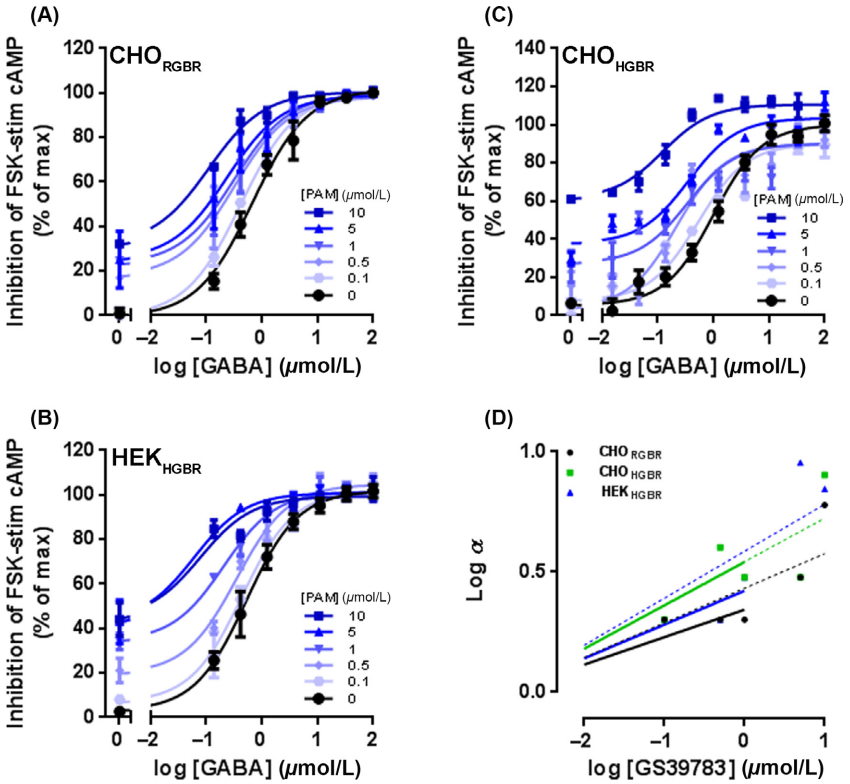

Figure 2. cAMP HTRF-measured effects of GS39783 on GABA-induced $GABA_B$R-mediated inhibition of forskolin-stimulated cAMP production. Concentration–response curves for GABA in the absence and in the presence of increasing concentration of allosteric ligand in CHO_{RGBR} (A), HEK_{HGBR} (B), or CHO_{HGBR} (C) cells line. (D) Linear regression plots were constructed from the logarithm of GS39783 concentration against the logarithm of the fold shift of the GABA EC_{50} (α). The solid and dashed trendlines were created by plotting the α values obtained with GS39783 at 0.1–1 μmol/L or 0.1–10 μmol/L, respectively. The data are means ± SEM of a typical experiment that was performed three times.

formation by GABA was fully antagonized by the competitive antagonist CGP54626, and no effect of GABA was observed in nontransfected CHO or HEK293 cells (data not shown).

Co-addition of 0.1–1 μmol/L of GS39783, resulted in a twofold leftward potency shift in GABA EC_{50} in the CHO_{RGBR} cells, and 5–10 μmol/L enhanced GABA EC_{50} ~3–6 fold (Fig. 2A, Table 2). We have assigned the potency shift observed in the presence of an allosteric modulator an 'α' value, where an α value >1 defines positive modulation, and an 'α' value <-1 defines negative modulation. Hence, in CHO_{RGBR} cells, 10 μmol/L GS39783 has an $\alpha = 6$ (Table 2). In HEK_{HGBR} and CHO_{RGBR} cells, 0.1–1 μmol/L and 5–10 μmol/L of GS39783 generated α values of ~2–3 and ~7–9, respectively (Fig. 2B and C; Table 2). Furthermore, GS39783 also exhibited significant intrinsic activity (~30% of GABA EC_{max}) in CHO_{RGBR}, HEK_{HGBR}, and CHO_{HGBR} cells when present at 0.5–10 μmol/L (Fig. 2A and B; Table 2). Correlation plots constructed from the fold shift of the GABA EC_{50} (α) in the presence of a given concentration of the modulator demonstrated that with regard to cAMP production, GS39783 exhibits similar PAM activity in cellular systems expressing either the rat or the human $GABA_B$R heterodimer (Fig. 2D, Table 3). Importantly, low micromolar concentration (0–1 μmol/L) showed significant PAM activity with $P = 0.0018$, 0.0023, and 0.0015 (*F*-test from nonzero slope) in CHO_{RGBR}, CHO_{HGBR}, and HEK_{HGBR}, respectively (Fig. 2D, Table 3). These results are in good agreement with GS39783 pharmacokinetics (Table 1) and in vivo efficacy (Paterson et al. 2008).

We next evaluated BHF177 in the CHO_{RGBR} cells. Submicromolar concentration (0.1–1 μmol/L) of BHF177 enhanced GABA potency by 2–3 fold (α = 2–3), whereas 5 μmol/L and 10 μmol/L generated α values of 5–6 (Fig. 3A, Table 2). In addition, BHF177 displayed significant intrinsic activity even at low micromolar concentrations and behaved almost as a full agonist when present at 10 μmol/L, activating the $GABA_B$R by ~80% of GABA EC_{max} (Fig. 3A, Table 2). In contrast, in HEK_{HGBR} and CHO_{HGBR} cells, BHF177 neither modulated nor promoted $GABA_B$R activity when present at 0.1–1 μmol/L (Fig. 3B and C, Table 2). Nevertheless, PAM activity

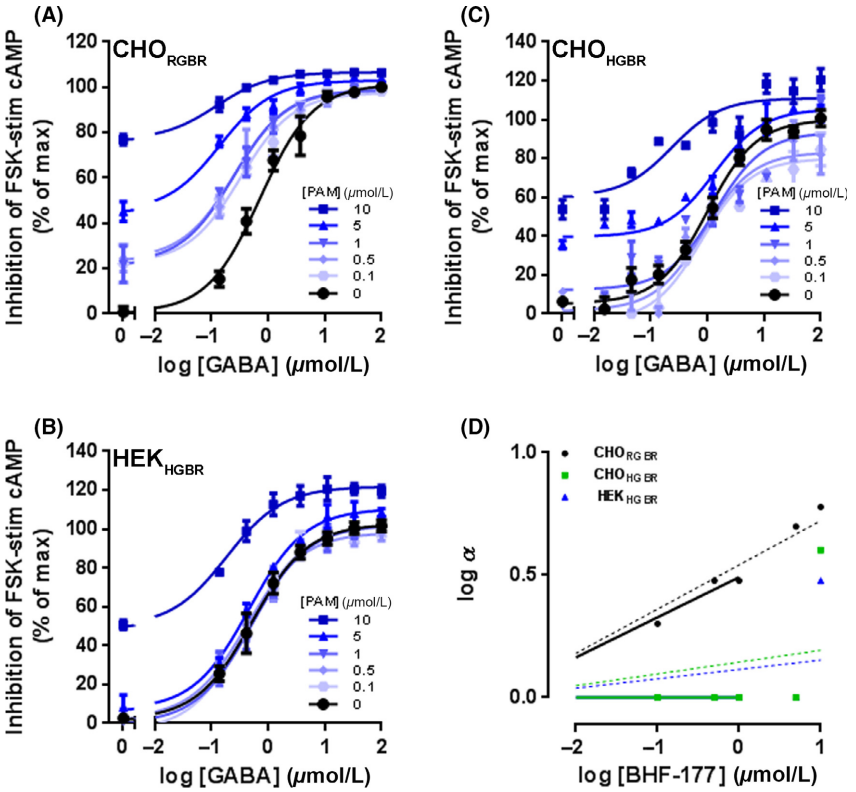

Figure 3. cAMP HTRF-measured effects of BHF177 on GABA-induced $GABA_BR$-mediated inhibition of forskolin-stimulated cAMP production. Concentration–response curves for GABA in the absence and in the presence of increasing concentration of allosteric ligand in CHO_{RGBR} (A), HEK_{HGBR} (B), or CHO_{HGBR} (C) cells line. (D) Linear regression plots were constructed from the logarithm of BHF177 concentration against the logarithm of the fold shift of the GABA EC_{50} (α). The solid and dashed trendlines were created by plotting the α values obtained with BHF177 at 0.1–1 μmol/L or 0.1–10 μmol/L, respectively. The data are means ± SEM of a typical experiment that was performed three times.

(α = 3–4) and significant intrinsic activity was observed at 10 μmol/L (Fig. 3B and C, Table 2). In addition, BHF177 at 10 μmol/L was found to significantly increase GABA efficacy to ~125% in HEK_{HGBR} (Fig. 3B; Table 2). Correlation plots constructed from the fold shift of the GABA EC_{50} (α) in the presence of a given concentration of the modulator demonstrated that low micromolar concentration exhibit significant PAM activity with P = 0.0001 (F-test from nonzero slope) in cells expressing the rat receptor (CHO_{RGBR}) (Fig. 3D, Table 3). These in vitro data are in good agreement with BHF177 pharmacokinetics (Table 1) and in vivo efficacy (Paterson et al. 2008). Interestingly, similar concentrations of BHF177 did not display PAM activity in cellular systems expressing the human receptor (HEK_{HGBR} and CHO_{HGBR}) suggesting that BHF177 might exhibit a distinct in vitro pharmacological profile depending on the composition of the $GABA_BR$ heterodimer.

NVP998 exhibited PAM activity (α=3) and displayed intrinsic activity (41 ± 4%) when present at the higher concentration (10 μmol/L) in the CHO_{RGBR} cells (Fig. 4A, Table 2). In contrast, low micromolar concentrations of this allosteric ligand (0.1–5 μmol/L) failed to enhance GABA EC_{50} or to activate the receptor in this cellular system (Fig. 4A and D, Table 2). These in vitro observations are in good agreement with the absence of an in vivo effect of NVP998 on nicotine self-administration (Fig. 1). However, in HEK_{HGBR} and in CHO_{HGBR} cells, NVP998 significantly enhanced GABA potency even when present at low micromolar concentration with P = 0.040 and 0.009 (F-test from nonzero slope), respectively (Fig. 4B–D, Table 3). Furthermore, in these cellular systems, 5 and 10 μmol/L of NVP998 displayed significant agonist activity (Table 2). Thus, as previously observed with BHF177, NVP998 exhibits system-dependent ago-PAM activity.

Although, these data confirm that GS39783, BHF177, and NVP998 display PAM activity at the $GABA_BR$; they also reveal the existence of cellular system-dependent effects suggesting that $GABA_BR$ allosteric ligands might exhibit species selectivity. Interestingly, although NVP998 and BHF177 both display species selectivity, they do so in

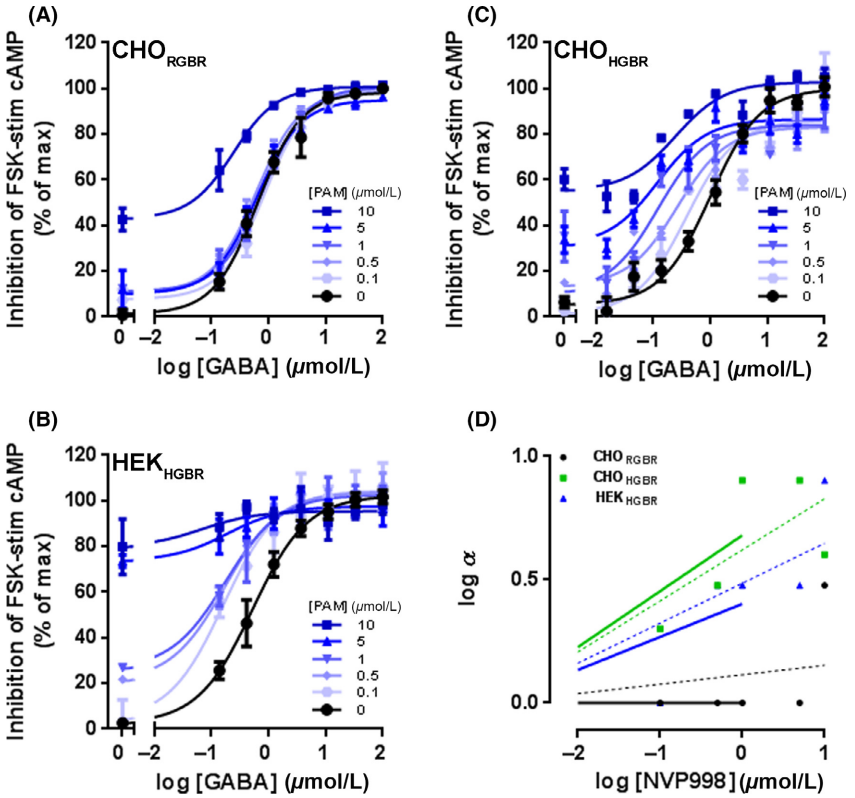

Figure 4. cAMP HTRF-measured effects of NVP998 on GABA-induced $GABA_B$R-mediated inhibition of forskolin-stimulated cAMP production. Concentration–response curves for GABA in the absence and in the presence of increasing concentration of allosteric ligand in CHO_{RGBR} (A), HEK_{HGBR} (B), or CHO_{HGBR} (C) cells line. (D) Linear regression plots were constructed from the logarithm of NVP998 concentration against the logarithm of the fold shift of the GABA EC_{50} (α). The solid and dashed trendlines were created by plotting the α values obtained with NVP998 at 0.1–1 μmol/L or 0.1–10 μmol/L, respectively. The data are means ± SEM of a typical experiment that was performed three times.

favor of different species; NVP998 exhibiting increased PAM activity at the human receptor, whereas BHF177 exhibited significant PAM activity at the rat receptor (Fig 3D and 4D).

Effects of GS39783 and analogs on $GABA_B$R-mediated mobilization of intracellular Ca^{2+}

Previous reports have demonstrated that the $GABA_B$R can promote increases in intracellular calcium concentrations $[Ca^{2+}]_i$ via the activation of either inositol-3 phosphate receptors (IP_3Rs) store-operated channels, or by directly interacting with voltage-gated $Ca_v1.3$ Ca^{2+} channel (Park et al. 2010; New et al. 2006; Meier et al. 2008). Therefore, we investigated the possibility that the aforementioned allosteric ligands can modulate $GABA_B$R-mediated increases in intracellular Ca^{2+} levels in the HEK_{HGBR} and the CHO_{RGBR} cells. As expected, addition of GABA induced a rise in $[Ca^{2+}]_i$ within 20–30 sec of GABA addition, reaching a maximal response at 45–50 sec after agonist addition, before returning to basal levels within 120 sec (data not shown).

As shown in Figures 5–7, addition of GABA resulted in a concentration-dependent increase in $[Ca^{2+}]_i$ with an EC_{50} value of 1.4 and 0.25 μmol/L in the CHO_{RGBR} and HEK_{HGBR} cells, respectively. These EC_{50} values correlate well with EC_{50} values obtained in the cAMP HTRF assay. The GABA-induced Ca^{2+} response was abolished by co-treatment with the competitive antagonist CGP54626 in a concentration-dependent manner and no response to $GABA_B$R agonists was observed in the parental CHO and HEK cell lines (data not shown).

In the CHO_{RGBR} cell line, 1, 5, and 10 μmol/L of GS39783, decreased GABA potency by two-, three-, and sixfold, respectively (Fig. 5A; Table 2). Similarly, in HEK_{HGBR} cells, GABA EC_{50} was decreased by threefold in the presence of 0.1 and 0.5 μmol/L of GS39783 and by 4–5 fold when the allosteric ligand was present at higher concentrations (Fig. 5B; Table 2). Thus, with regard to changes in $[Ca^{2+}]$i, GS39783 decreases GABA potency

and as such behaves as a negative allosteric modulator (NAM) in both cell lines. Interestingly, in the absence of GABA, addition of 5 and 10 μmol/L of GS39783 induced a rise in $[Ca^{2+}]_i$ in both cellular systems (~23% and ~60%, respectively) (Fig. 5A and B; Table 2). However, similar activity was also observed in parental CHO and HEK293 cells suggesting that the GS39783-induced rise in $[Ca^{2+}]_i$ is not $GABA_BR$ specific (data not shown). As observed in the cAMP assay (Fig. 2D), correlation plots constructed from the fold shift of the GABA EC_{50} (α) in the presence of a given concentration of the modulator demonstrated that GS39783 in vitro NAM activity was comparable in CHO_{RGBR} and HEK_{HGBR} cells (Fig. 5C, Table 3). Nevertheless, low micromolar concentration (0.1–1 μmol/L) only exhibited significant NAM activity with $P = 0.0009$ (*F*-test from nonzero slope) in cells expressing the human $GABA_BR$ heterodimer (HEK_{HGBR}) (Fig. 5C, Table 3). Thus, together with the cAMP assay data, these observations suggest that GS39783 displays signaling pathway-specific activity.

In the CHO_{RGBR} cells, BHF177 at 10 μmol/L was found to exhibit PAM activity ($\alpha = 4$) as well as some degree of intrinsic activity (12 $\pm$ 3%), whereas lower concentrations did not significantly affect $GABA_BR$-mediated changes in $[Ca^{2+}]_i$ (Fig. 6A, Table 2). Conversely, in the HEK_{HGBR} cells, BHF177 at 0.1–5 μmol/L exhibited weak negative allosteric modulator (NAM) activity as indicated by a rightward shift of the GABA CRC (Fig. 6B; Table 2). Nevertheless, correlation plots constructed from the fold shift of the GABA EC_{50} (α) in the presence of a given concentration of the modulator demonstrated that with regard to $[Ca^{2+}]_i$ mobilization, BHF177 does not exhibit significant PAM/NAM activity in cellular systems expressing either the rat or the human $GABA_BR$ heterodimer (Fig. 2D, Table 3). These data indicate that BHF177 has differential effects on $GABA_BR$-mediated changes in intracellular calcium levels versus cAMP levels suggesting that BHF177 not only exhibits species selectivity but also pathway-selective behavior.

In the CHO_{RGBR} cell line, 0.1, 0.5, and 1 μmol/L of NVP998 decreased GABA potency by three-, four-, and sixfold, respectively (Fig. 7A; Table 2). In contrast, at 5 and 10 μmol/L, the allosteric ligand exhibited PAM activity and enhanced GABA potency by 2–3 fold. The correlation plot constructed from the fold shift of the GABA EC_{50} (α) in the presence of a given concentration of the modulator demonstrated that at low micromolar concentrations NVP998 exhibits significant NAM activity with $P = 0.0001$ (*F*-test from nonzero slope) in cells expressing the rat $GABA_BR$ receptor (Fig. 7C, Table 3). These in vitro observations correlate well with the absence of an in vivo effect of NVP998 on nicotine self-administration (Fig. 1). In HEK_{HGBR} cells, NVP998 at 10 μmol/L exhibited PAM activity ($\alpha = 3$) (Fig. 7B; Table 2) and displayed intrinsic agonist activity (~20%). In contrast, lower concentrations of the allosteric ligand did not affect $GABA_BR$ activity in this cellular assay system.

Effects of GS39783 and analogs on $GABA_BR$-mediated $ERK_{1/2}$ phosphorylation

It has been reported that $GABA_BR$ activation leads to the activation of the $ERK_{1/2}$ signaling cascade. $ERK_{1/2}$ activation occurs via the $GABA_BR2$ subunit coupling to $G_{i/o}$ proteins by releasing the $G_{\beta\gamma}$ subunit (Tu et al. 2007). In addition, a recent report indicated that the $GABA_BR$ can increase $ERK_{1/2}$ phosphorylation by directly interacting with, and activating the Ca(v)1.3 channel (Im and Rhim 2012). Thus, we next investigated the possibility that the allosteric ligands would also modulate $GABA_BR$-mediated $ERK_{1/2}$ phosphorylation. We first studied the effect of a saturating concentration of GABA (100 μmol/L) on $ERK_{1/2}$ phosphorylation in the CHO_{RGBR} and HEK_{HGBR} cells using the "*In cell*" western blot technique to determine the time point at which maximal $ERK_{1/2}$ phosphorylation occurs after receptor activation. Addition of GABA induced a rapid and transient increase in $ERK_{1/2}$ phosphorylation peaking at 5 min, with no changes in total $ERK_{1/2}$ expression in both cellular systems (Fig. S1). Importantly, no response to the $GABA_BR$ agonist was observed in the parental CHO or HEK293 cell line (data not shown).

To investigate the effect of the allosteric ligands on $GABA_BR$-mediated $ERK_{1/2}$ activation, both cellular systems were stimulated with GABA alone or in the presence of the modulator for 5 min, and $ERK_{1/2}$ phosphorylation was measured using Cellul'erk HTRF assay. As anticipated, addition of GABA resulted in a concentration-dependent increase in phospho-ERK with an EC_{50} value of 0.56 μmol/L and 0.65 μmol/L in CHO_{RGBR} and HEK_{HGBR} cells, respectively (Fig. 8). We next investigated the effect of the allosteric ligands on $GABA_BR$-mediated $ERK_{1/2}$ phosphorylation.

In CHO_{RGBR} cells, 1 μmol/L GS39783 alone did not promote $ERK_{1/2}$ phosphorylation, whereas it enhanced GABA potency by fivefold when present at 10 μmol/L (Fig. 8A; Table 2). In addition, in this cellular system, the maximal stimulation obtained by saturating concentrations of GABA was significantly increased in the presence of 1 and 10 μmol/L of the allosteric ligand (~120%) (Fig. 8A; Table 2). In HEK_{HGBR} cells, GS39873 enhanced GABA potency by two- and eightfold and exhibited significant intrinsic activity, activating $ERK_{1/2}$ by 52% $\pm$ 7 and 63% $\pm$ 14 when present at 1 and 10 μmol/L, respectively (Fig. 8D, Table 2). In the CHO_{RGBR} cells, 1 and 10 μmol/L of BHF177 enhanced GABA potency by two- and threefold, respectively (Fig. 8B; Table 2). Also, the

Table 2. Effects of allosteric ligands on potency and efficacy of GABA-induced $GABA_BR$-mediated cellular responses in CHO_{RGBR} (Rat) or HEK_{HGBR}, CHO_{HGBR} (Hu) cells. Concentration–response curves for GABA were determined in the absence or presence of the indicated concentration of allosteric modulator. The potency shift values (α) are indicated, and the intrinsic activity and the maximal stimulation are expressed in percent of the effects obtained with a saturating concentration of GABA (100 μmol/L) alone.

		GS39783						BHF-177						NVP998					
	(Drug)	α		Int act (%)		*E*max (%)		α		Int act (%)		*E*max (%)		α		Int act (%)		*E*max (%)	
	(μmol/L)	Rat	Hu	Rat	Hu	Rat	Hu	Rat	Hu	Rat	Hu	Rat	Hu	Rat	Hu	Rat	Hu	Rat	Hu
cAMP	0	1	1, 1	−1 ± 4	0 ± 5, 5 ± 2	100 ± 2	103 ± 3, 100 ± 2	1	1, 1	−1 ± 4	0 ± 5, 5 ± 2	100 ± 2	103 ± 3, 100 ± 3	1	1, 1	−1 ± 4	0 ± 5, 5 ± 2	100 ± 2	103 ± 3, 100 ± 3
assay	0.1	2	2, 2	9 ± 3	5 ± 3, 7 ± 3	95 ± 2	101 ± 4, 90 ± 4	2	1, 1	16 ± 4*	−9 ± 4, −4 ± 5	101 ± 4	100 ± 2, 80 ± 3**	1	3, 2	8 ± 3	−3 ± 3, 1 ± 4	101 ± 1	103 ± 4, 86 ± 5
	0.5	2	2, 4	28 ± 5*	17 ± 3*, 4 ± 3	95 ± 3	99 ± 4, 90 ± 4	3	1, 1	20 ± 4*	−3 ± 5, 2 ± 3	100 ± 2	99 ± 2, 83 ± 3*	1	3, 3	9 ± 5	15 ± 3, 13 ± 3	100 ± 3	102 ± 4, 83 ± 3*
	1	2	3, 3	35 ± 6**	31 ± 3**, 27 ± 3**	95 ± 3	102 ± 3, 92 ± 4	3	1, 1	18 ± 8	−4 ± 4, 13 ± 3	101 ± 2	103 ± 2, 93 ± 3	1	3, 8	12 ± 6	22 ± 3*, 11 ± 5	99 ± 4	100 ± 2, 84 ± 5
	5	3	9, 3	29 ± 5**	32 ± 6*, 38 ± 3**	95 ± 2	98 ± 5, 110 ± 3	5	1, 1	28 ± 13	2 ± 5, 40 ± 2**	107 ± 1	111 ± 2, 105 ± 2	1	3, 8	8 ± 5	74 ± 6**, 31 ± 4**	100 ± 2	101 ± 3, 87 ± 4
	10	6	7, 8	30 ± 4**	38 ± 4**, 61 ± 3**	96 ± 1	101 ± 2, ±3	6	3, 4	78 ± 2**	34 ± 4**, 60 ± 5**	106 ± 3	123 ± 3**, 111 ± 4	3	8, 4	41 ± 4**	82 ± 4**, 55 ± 2**	101 ± 2	102 ± 3, 102 ± 3
Calcium	0	1	1	−3 ± 3	1 ± 3	100 ± 4	100 ± 3	1	1	−3 ± 3	1 ± 3	100 ± 4	100 ± 3	1	1	−3 ± 3	1 ± 3	100 ± 4	100 ± 3
assay	0.1	1	−3	2 ± 3	0 ± 3	74 ± 3**	96 ± 4	1	−2	−1 ± 2	−2 ± 3	89 ± 4	102 ± 5	−3	1	0 ± 2	2 ± 5	90 ± 5	100 ± 5
	0.5	1	−3	0 ± 3	−2 ± 4	74 ± 4*	94 ± 4	2	−3	−1 ± 3	−1 ± 5	102 ± 3	105 ± 9	−4	1	−3 ± 2	−1 ± 5	94 ± 5	93 ± 5
	1	−2	−5	2 ± 3	−2 ± 6	106 ± 5	100 ± 4	1	−2	2 ± 2	5 ± 3	98 ± 4	94 ± 4	−6	1	0 ± 2	2 ± 4	84 ± 6	100 ± 6
	5	−3	−4	23 ± 3*	23 ± 4*	106 ± 3	110 ± 4	2	−2	−3 ± 3	−0 ± 7	101 ± 3	111 ± 10	3	1	−2 ± 3	25 ± 5*	67 ± 3**	108 ± 5
	10	−6	−4	64 ± 3**	60 ± 5**	126 ± 5*	120 ± 4*	4	1	12 ± 3*	3 ± 4	101 ± 3	100 ± 4	2	3	1 ± 3	18 ± 5*	91 ± 4	103 ± 4
ERK	0	1	1	4 ± 4	2 ± 3	100 ± 4	98 ± 4	1	1	4 ± 4	2 ± 3	100 ± 4	98 ± 4	1	1	4 ± 4	2 ± 3	100 ± 4	98 ± 4
assay	0.1	nd	nd	nd	nd	nd	nd	nd	nd	nd	Nd	nd	nd	nd	nd	nd	nd	nd	nd
	0.5	nd	nd	nd	nd	nd	nd	nd	nd	nd	nd	nd	nd	nd	nd	nd	nd	nd	nd
	1	1	2	−3 ± 3	52 ± 7**	123 ± 5*	97 ± 7	2	5	−3 ± 4	12 ± 6	105 ± 2	102 ± 6	1	5	−6 ± 4	44 ± 6**	127 ± 2**	105 ± 6
	5	nd	nd	nd	nd	nd	nd	nd	nd	nd	nd	nd	nd	nd	nd	nd	nd	nd	nd
	10	5	8	6 ± 2	63 ± 14**	122 ± 4*	98 ± 4	3	5	4 ± 1	30 ± 5*	117 ± 1*	106 ± 9	3	5	20 ± 1*	51 ± 5**	128 ± 1**	98 ± 9
CellKey	0	1	nd	−2 ± 1	nd	101 ± 1	nd	1		−2 ± 1	nd	101 ± 1	nd	1	nd	−2 ± 1	nd	101 ± 1	nd
assay	0.1	nd	nd	nd	nd	nd	nd	nd		nd	nd	nd	nd	nd	nd	nd	nd	nd	nd
	0.5	nd	nd	nd	nd	nd	nd	nd		nd	nd	nd	nd	nd	nd	nd	nd	nd	nd
	1	1	nd	−2 ± 2	nd	90 ± 3	nd	2		−5 ± 3	nd	112 ± 3*	nd	1	nd	−2 ± 2	nd	94 ± 2	nd
	5	nd	nd	nd	nd	nd	nd	nd		nd	nd	nd	nd	nd	nd	nd	nd	nd	nd
	10	15	nd	15 ± 4*	nd	118 ± 2**	nd	52		36 ± 5**	nd	128 ± 5**	nd	15	nd	20 ± 3**	nd	104 ± 4	nd

The data shown are means ± SEM. Statistic by two-tailed *t*-test: $*P < 0.05$, $**P < 0.01$.

Table 3. Linear regression analyses comparing the logarithm of the allosteric ligand concentration against the logarithm of the fold shift of the GABA EC_{50} (α) to predict PAM activity of GS39783 and analogs in CHO_{RGBR}, CHO_{HGBR}, or HEK_{HGBR}, cells. Linear regression analyses were also performed with in vivo relevant dose of the different PAMs (0–1 μmol/L).

			GS39783		BHF177		NVP998	
Assay	Cell line	(drug) (μmol/L)	Slope	*P*	Slope	*P*	Slope	*P*
cAMP assay	CHO_{RGBR}	0–1	0.1143 ± 0.0107	0.0018*	0.1637 ± 0.0059	0.0001*	–	–
		0–10	0.1440 ± 0.0166	0.0003*	0.1805 ± 0.0069	<0.0001*	0.0382 ± 0.0248	0.1855
	CHO_{HGBR}	0–1	0.1804 ± 0.0185	0.0023*	–	–	0.2267 ± 0.0386	0.0099*
		0–10	0.1808 ± 0.0189	0.0002*	0.0482 ± 0.0314	0.1855	0.2071 ± 0.0260	0.0005*
	HEK_{HGBR}	0–1	0.1403 ± 0.0125	0.0015*	–	–	0.1340 ± 0.0386	0.0403*
		0–10	0.1952 ± 0.0227	0.0004*	0.0382 ± 0.0248	0.1855	0.1620 ± 0.0273	0.0019*
Calcium assay	CHO_{RGBR}	0–1	−0.0445 ± 0.0287	0.2196	0.0426 ± 0.0728	0.6176	−0.2422 ± 0.0093	0.0001*
		0–10	−0.1157 ± 0.0319	0.0152*	0.1190 ± 0.0606	0.1214	−0.0389 ± 0.0758	0.6298
	HEK_{HGBR}	0–1	−0.2139 ± 0.0160	0.0009*	−0.1316 ± 0.0477	0.1104	–	–
		0–10	−0.1796 ± 0.0151	<0.0001*	−0.0349 ± 0.0640	0.6146	0.0382 ± 0.0248	0.1855
ERK assay	CHO_{RGBR}	0–1	–	–	0.1003	–	–	–
		0–10	0.1118 ± 0.05931	0.2	0.1125 ± 0.0064	0.0033*	0.0763 ± 0.0404	0.2
	HEK_{HGBR}	0–1	0.1003 ± 0.0	–	0.233	–	0.233	–
		0–10	0.1806 ± 0.04257	0.0513	0.1957 ± 0.0197	0.0101*	0.1957 ± 0.0197	0.0101*

*Significant deviation from zero (*F*-test for non-zero slope, *P*-value).

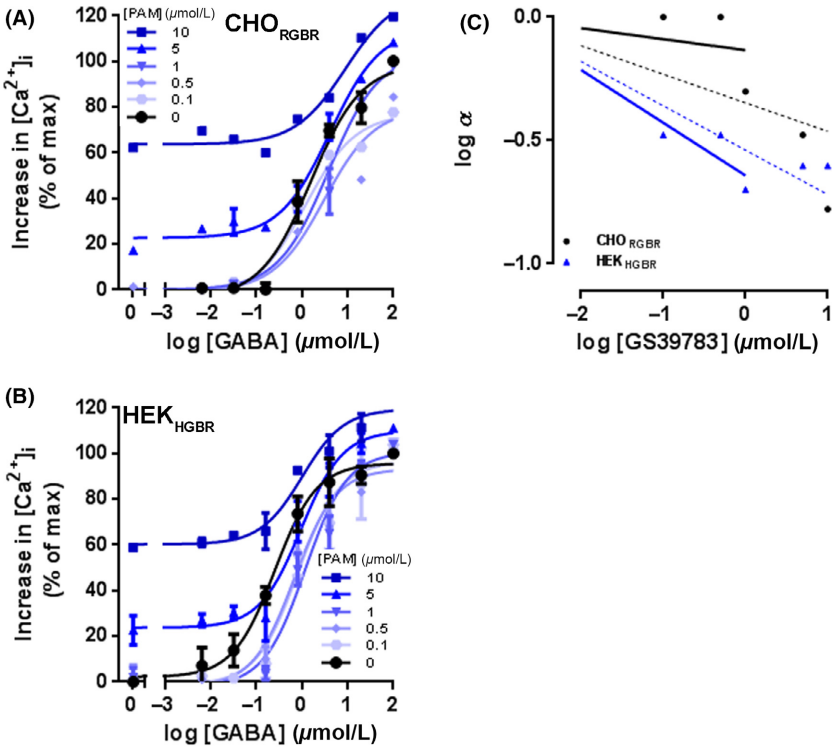

Figure 5. Potentiation of GABA-induced $GABA_B$R-mediated intracellular calcium mobilization by GS39783. Concentration–response curves for GABA in the absence or presence of increasing concentrations of allosteric ligand in CHO_{RGBR} (A) or HEK_{HGBR} (B) cell lines. (C) Linear regression plots were constructed from the logarithm of GS39783 concentration against the logarithm of the fold shift of the GABA EC_{50} (α). The solid and dashed trendlines were created by plotting the α values obtained with GS39783 at 0.1–1 μmol/L or 0.1–10 μmol/L, respectively. The data are means ± SEM of a typical experiment that was performed three times.

maximal stimulation obtained by a saturating concentration of GABA was significantly increased in the presence of 10 μmol/L of BHF177 (117% ± 7). In HEK_{HGBR} cells, BHF177 enhanced GABA EC_{50} by fivefold at 1 and 10 μmol/L, and also displayed significant intrinsic activity at the highest concentration (30% ± 6) (Fig. 8E; Table 2).

In the CHO_{RGBR} cells, NVP998 did nor enhance GABA potency at 1 μmol/L, whereas the allosteric ligand enhanced GABA EC_{50} by threefold at 10 μmol/L (Fig. 5C, Table 2). In this cellular system, NVP998 also displayed significant intrinsic activity at 10 μmol/L and activated $ERK_{1/2}$ by 20% ± 1 (Fig. 5C, Table 2). In addition, as observed with the other allosteric ligands, the maximal stimulation obtained by saturating concentrations of GABA was significantly increased in the presence of 1 and 10 μmol/L of NVP998 (~130%) (Fig. 5C, Table 2). In HEK_{HGBR} cells, 1 and 10 μmol/L of NVP998 enhanced GABA EC_{50} by fivefold, and exhibited significant intrinsic activity (44% ± 6 and 51% ± 5, respectively) (Fig. 8F; Table 2). Correlation plots constructed from the fold shift of the GABA EC_{50} (α) in the presence of a given concentration of the modulator demonstrated that with regard to ERK activation, (i) BHF177 displays significant PAM activity in both CHO_{RGBR} and HEK_{HGBR} with $P = 0.0033$ and 0.0101 (*F*-test from nonzero slope), respectively, (ii) NVP998 exhibits significant PAM activity only in HEK_{HGBR} with $P = 0.010$ (*F*-test from nonzero slope), and (iii) GS39783 did not demonstrate significant PAM activity in these cellular systems (Fig. 8G, Table 3). Together with our previous observations these data confirm that $GABA_BR$ allosteric ligands not only exhibit functional selectivity but their activities are also context-dependent.

Effects of GS39783 and analogs on $GABA_BR$ desensitization

Since the allosteric ligands display intrinsic activity, they may induce $GABA_BR$ desensitization. Thus, we further investigated the effect of GS39783, BHF177 and NVP998 on $GABA_BR$ desensitization using a label free technology (CellKey system) which allows noninvasive bioimpedance-based measurement of an integrated

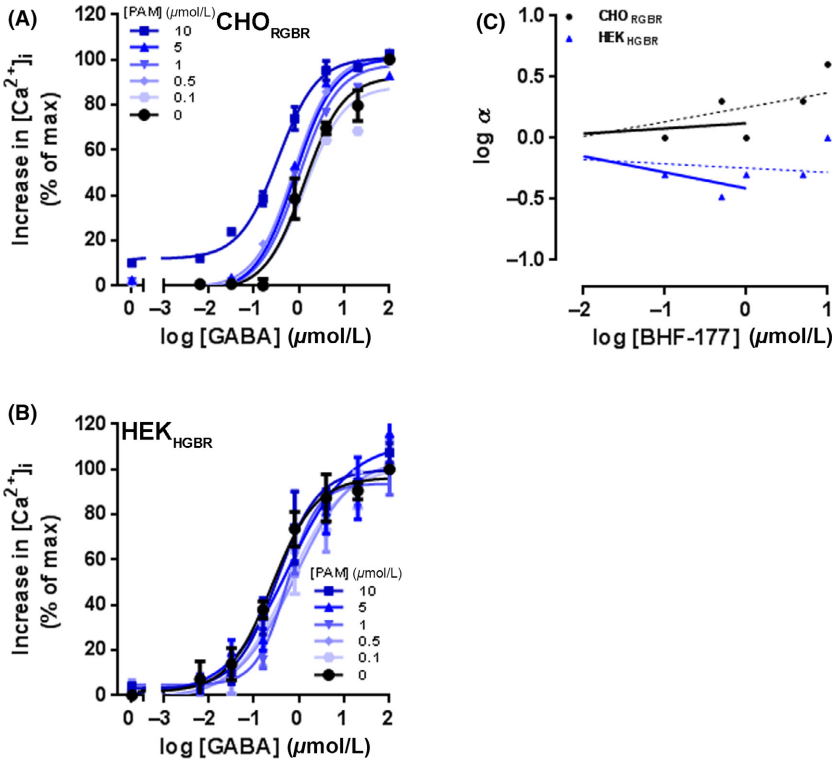

Figure 6. Potentiation of GABA-induced $GABA_BR$-mediated intracellular calcium mobilization by BHF177. Concentration–response curves for GABA in the absence or presence of increasing concentrations of allosteric ligand in CHO_{RGBR} (A) or HEK_{HGBR} (B) cell lines. (C) Linear regression plots were constructed from the logarithm of BHF177 concentration against the logarithm of the fold shift of the GABA EC_{50} (α). The solid and dashed trendlines were created by plotting the α values obtained with BHF177 at 0.1–1 μmol/L or 0.1–10 μmol/L, respectively. The data are means ± SEM of a typical experiment that was performed three times.

cellular response (Ciambrone et al. 2004). In this assay, GABA induced concentration-dependent changes in cellular impedance with an EC_{50} value of 0.57 μmol/L in CHO_{RGBR}. In agreement with our previous data, the allosteric ligands exhibited PAM activity and displayed intrinsic activity when present at 10 μmol/L (Fig. 9A–C, Table 2). It is well established that following a first stimulation, GPCRs that undergo desensitization display reduced responsiveness to a second stimulation with an agonist. Therefore, CHO_{RGBR} cells were stimulated for 20 min with 1 or 10 μmol/L of the allosteric ligands, or 1 or 100 μmol/L of the orthosteric agonist GABA. Subsequently, the ligand-containing medium was removed; the cells were washed three times and further incubated in assay buffer for 30 min before being stimulated a second time with a GABA EC_{90} (~5 μmol/L). In CHO_{RGBR} cells exposed to 100 μmol/L of GABA, the response to a second stimulation was significantly attenuated (Fig. 9D). In good agreement with previous reports (Gjoni and Urwyler 2008), these data suggest that high concentrations of GABA induce $GABA_BR$ desensitization. In contrast, in CHO_{RGBR} cells exposed to the allosteric ligands, the variation of cellular impedance induced by the second stimulation was not decreased when compared to the control (Fig. 9E) suggesting that the allosteric ligands do not promote $GABA_BR$ desensitization.

Discussion

In this study, we have performed extensive in vitro pharmacological characterization of the structurally related $GABA_BR$-positive allosteric modulators (PAMs), GS39783, BHF177, and NVP998. We have also examined the effects of NVP998 on nicotine self-administration in the rat in order to compare these effects to our previously published data describing the effects of GS39783, and BHF177 on nicotine self-administration (Paterson et al. 2008; Vlachou et al., 2011). The main findings are that each of the $GABA_BR$ allosteric ligands evaluated exhibit functional as well as receptor ortholog selectivity, indicating that even minor structural changes can have profound effects on

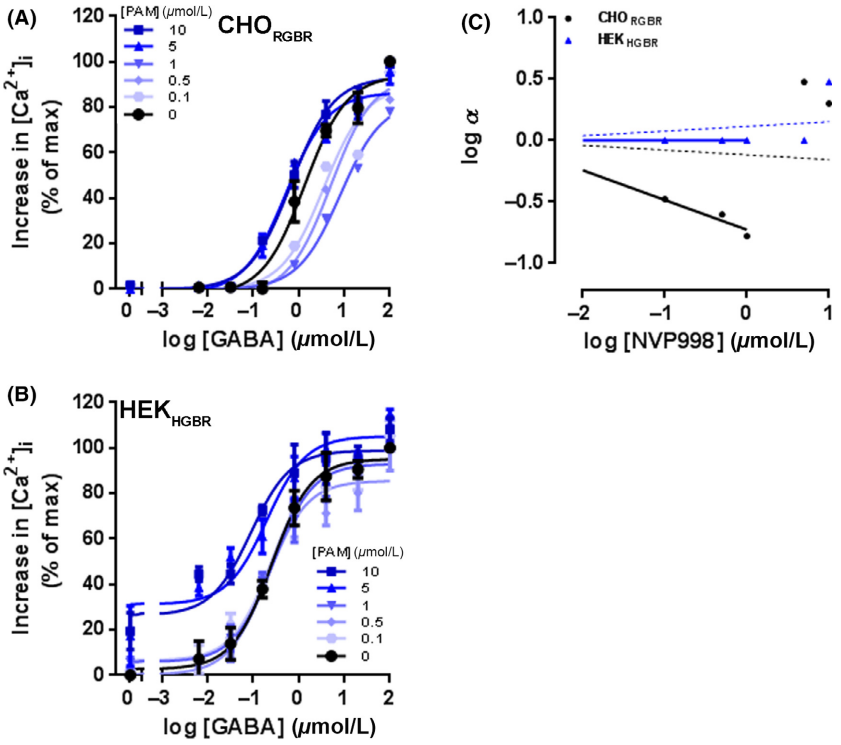

Figure 7. Potentiation of GABA-induced $GABA_BR$-mediated intracellular calcium mobilization by NVP998. Concentration–response curves for GABA in the absence or presence of increasing concentrations of allosteric ligand in CHO_{RGBR} (A) or HEK_{HGBR} (B) cell line. (C) Linear regression plots were constructed from the logarithm of NVP998 concentration against the logarithm of the fold shift of the GABA EC_{50} (α). The solid and dashed trendlines were created by plotting the α values obtained with NVP998 at 0.1–1 μmol/L or 0.1–10 μmol/L, respectively. The data are means ± SEM of a typical experiment that was performed three times.

pathway and species selectivity; critical properties that need to be considered as early as possible in the drug discovery process.

A decade ago GS39783, and structural analogs BHF177, and NVP998, were the first positive allosteric modulators (PAMs) of the $GABA_BR$ to be described. These molecules were found to potentiate GABA-stimulated guanosine 5′-O-(3-[(35)S]thiotriphosphate) ($[^{35}S]GTP\gamma S$) binding to membranes generated from CHO cells heterologously expressing the human/rat $GABA_BR$ (CHO_{RGBR}), exhibiting maximal effect at 10 μmol/L (Urwyler et al. 2003; Guery et al. 2007). More recently, we have demonstrated that BHF177 and GS39783 are effective in decreasing nicotine self-administration in rats (Paterson et al. 2008). Interestingly, the in vivo efficacy of GS39783 was equivalent to BHF177 only when co-administered with a subeffective dose of the $GABA_BR$ agonist CGP44532. Here, we demonstrate that NVP998 when administered either p.o or i.c.v had no effect on nicotine self-administration under fixed- and progressive-ratio schedules of

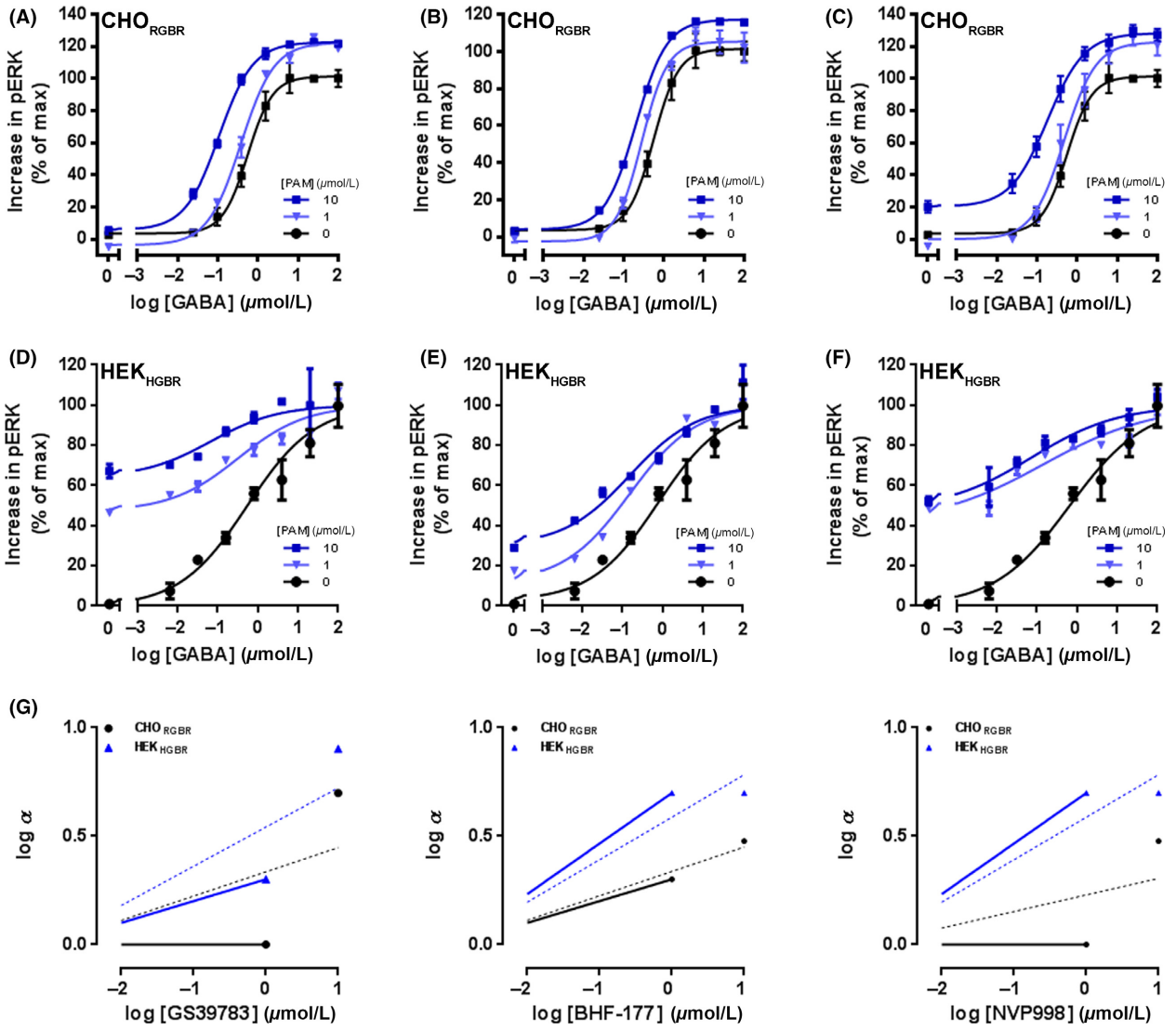

Figure 8. Modulation of $GABA_BR$-mediated $ERK_{1/2}$ phosphorylation by GS39783 and analogs. The graphs A–F show representative concentration–response curves for GABA in the Cellul'erk HTRF assay either in the absence or in the presence of 1 or 10 μmol/L of the specified allosteric ligand. The data points are normalized to the maximal effect of GABA alone. The responses were measured in either CHO_{RGBR} (A, C, and E) or HEK_{HGBR} (B, D, F) cell lines. (G) Linear regression plots were constructed from the logarithm of the allosteric ligand concentration against the logarithm of the fold shift of the GABA EC_{50} (α). The solid and dashed trendlines were created by plotting the α values obtained with allosteric ligand at 0–1 μmol/L or 0–10 μmol/L, respectively. The data are means ± SEM of a typical experiment that was performed three times.

reinforcement, suggesting that this compound had no effect on the reinforcing and motivational aspects of self-administered nicotine. Thus, despite the structural similarities, reported in vitro PAM activity (Urwyler et al. 2001), equivalent oral bioavailability, and similar brain exposure (Table 1), these $GABA_BR$ PAMs exhibit distinct in vivo efficacies.

It is now well accepted that different ligands acting at the same receptor subtype can activate/modulate distinct patterns of downstream responses, a phenomenon referred to as "functional selectivity", or "ligand bias". With this in mind and as the $GABA_BR$ possesses pleiotropic signaling capacity (Bettler and Tiao 2006), we hypothesized that differences in $GABA_BR$ allosteric modulator behavior toward specific signaling pathways may account for the dissimilarities observed in their efficacy in rat model of nicotine addiction. To test this hypothesis, we characterized the in vitro pharmacological profile of GS39783, BHF177, and NVP998 by investigating their effect on GABA-induced $GABA_BR$-mediated; (i) changes in intracellular cAMP levels; (ii) $[Ca^{2+}]_i$ mobilization; and (iii) $ERK_{1/2}$ phosphorylation. Since we used the rat as a preclinical model, and GS39783, BHF177, and NVP998 have previously been demonstrated to bind to the transmembrane domain of the $GABA_BR2$ subunit (Binet et al. 2004), we used CHO_{RGBR} cells expressing the human $GABA_BR1b$ and the rat $GABA_BR2$ subunits. Importantly, the GABA half-maximal response (EC_{50}) values obtained in the three distinct cell-based functional assays were found to correlate well with those previously reported in the literature (Urwyler et al. 2001). In good agreement with previous reports, 10 μmol/L of GS39783, BHF177, and NVP998 increased GABA potency in the cAMP assay performed with CHO_{RGBR} (Urwyler et al. 2003; Guery et al. 2007). Importantly, in this assay, BHF177 and GS39783 also displayed significant PAM activity at concentrations found in the rat brain (0.1–1 μmol/L), enhancing GABA EC_{50} by 2–3 fold (Table 3). In contrast, NVP998, did not demonstrate PAM activity at similar concentrations. Furthermore, GS39783 and BHF177 also exhibited significant intrinsic agonist activity in this assay (Fig. 2; Table 2), whereas NVP998 did not demonstrate

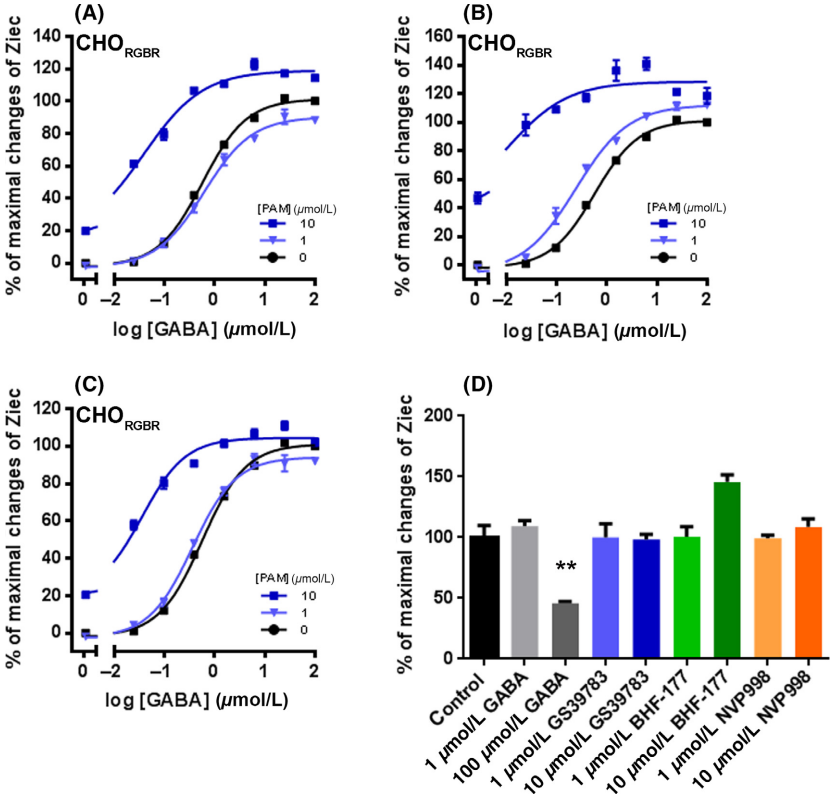

Figure 9. Characterization of $GABA_BR$ PAM effects on receptor desensitization using the CellKey assay. Concentration–response curves for GABA in the absence or presence of GS39783 (A), BHF177 (B) and NVP998 (C) in CHO_{RGBR}. D, Concentration–response curves for GABA in the absence or presence of increasing concentrations of allosteric ligand in CHO_{RGBR} (A) or HEK_{HGBR} (B) cell line. (C) Effect of GS39783, BHF177, and NVP998 on $GABA_BR$ desensitization. The data are means ± SEM of a typical experiment that was performed three times.

ago-allosteric modulator activity. Interestingly, the CellKey assay data revealed that in contrast to the orthosteric agonist, the allosteric ligands can activate the $GABA_BR$ without inducing receptor desensitization, a phenomenon involved in the development of tolerance. The $[Ca^{2+}]_i$ mobilization assay revealed additional differences in the behavior of the allosteric ligands in the CHO_{RGBR} cells. Indeed, in this assay, low micromolar concentrations of GS39783 and BHF177 did not significantly affect GABA potency, whereas low micromolar concentrations of NVP998 displayed significant NAM activity resulting in a decrease in GABA EC_{50}. Finally, in the $ERK_{1/2}$ activation assay, low micromolar concentrations (0.1–1 μmol/L) of GS39783 and NVP998 did not affect GABA potency, whereas BHF177 displayed PAM activity.

These results suggest that $GABA_BR$ allosteric ligands might exhibit distinct pathway-specific activity, highlighting the complexity of allosteric ligand behavior. Furthermore, these in vitro data indicate that in contrast to GS39783 and BHF177, NVP998 at the concentrations we observed in the rat brain, do not enhance GABA-induced cAMP nor ERK signaling and negatively modulated the GABA-mediated increase in $[Ca^{2+}]_i$. Together with our pharmacokinetics data, the NVP998 in vitro pharmacological profile in the CHO_{RGBR} cell line may explain the absence of effects on nicotine self-administration in rat. Thus, when comparing the in vitro profile of GS39783 and its analogs to their in vivo efficacy, our results suggest that allosteric ligands displaying an in vitro pharmacological profile similar to BHF177 may represent compounds that would be predicted to exhibit the desired in vivo properties.

In addition to functional selectivity, our studies also revealed that, GS39783, BHF177, and NVP998 may exhibit species-specific pharmacology. This characteristic has been previously described for numerous GPCR ligands including those that modulate adrenergic receptors, histamine receptors and GPR35 (Jenkins et al. 2012; Neetoo-Isseljee et al. 2013) as well as for allosteric modulators of the mGluR1 receptor, another family C GPCR (Knoflach et al. 2001). In agreement with previous reports demonstrating the effects of GS39783 in rat versus human $GABA_BR$ cellular systems (Urwyler et al. 2003), we found that this allosteric ligand displays similar efficacy in the cAMP assay in CHO_{RGBR}, in CHO_{HGBR}, and in HEK_{HGBR} cells. On the other hand, BHF177 and NVP998 both displayed species-specific behaviors. Indeed, in the cAMP assay, low micromolar concentrations (0.1–1 μmol/L) of BHF177 increased GABA potency in the CHO_{RGBR} but not in the CHO_{HGBR} nor in HEK_{HGBR} cells. Interestingly, in the same assay, NVP998 displayed alternate species-selectivity. Indeed, NVP998 enhanced GABA EC_{50} at low micromolar concentrations and exhibited strong intrinsic activity in CHO_{HGBR} and HEK_{HGBR} cells, whereas its ago-PAM activity was only observed at the highest concentration tested in the CHO_{RGBR}. Importantly, as noted above, the in vitro activity profile of these compounds together with their in vivo plasma and brain levels correlates well with their efficacy (BHF177), or lack thereof (NVP998) in a rat model of nicotine dependence. Since the in vitro pharmacological profile of NVP998 at the human receptor is comparable to that of BHF177 at the rat receptor, it may still represent a useful molecule for the development of $GABA_BR$-targeted therapy for nicotine addiction. However, in order for a molecule like NVP998 to progress in the drug development process, it would require evaluation in an alternative preclinical model such as nonhuman primates (Le Foll et al.; 2007), assuming species-selectivity is not an issue.

In conclusion, our studies demonstrate that functional and species-selectivity are operational at a $GABA_BR$ allosteric site, and that these phenomena have profound implications for drug discovery targeting the $GABA_BR$. Therefore, significant consideration must be given in the selection of appropriate ligands to progress in the drug discovery and development process. Importantly, we show that in vitro pharmacological profiling of $GABA_BR$ allosteric ligands can be predictive of in vivo efficacy in a preclinical rat model of nicotine addiction. Hence, parallel screening against receptor orthologs (human and preclinical model species) using a multi cell-based assay platform provides an ideal framework for selecting compounds with therapeutically appropriate profiles and will help bridge the gap between in vitro and in vivo compound efficacy.

Acknowledgements

We thank Dr. Wolfgang Froestl for insightful and helpful discussion. This work was supported by National Institutes of Health grant U19 DA026838.

Author Contributions

Participated in research design: Sturchler, Li, Markou, and McDonald. *Conducted experiments*: Sturchler, Li, Ladino. *Performed data analysis*: Sturchler, Li, Markou, and McDonald. *Wrote or contributed to the writing of the manuscript*: Sturchler, Li, Kaczanowska, Markou, Cameron, Finn, Griffin, and McDonald.

Disclosures

None declared.

References

Bettler B, Tiao JY (2006). Molecular diversity, trafficking and subcellular localization of GABAB receptors. Pharmacol Ther 110: 533–543.

Binet V, Brajon C, Le Corre L, Acher F, Pin JP, Prezeau L (2004). The heptahelical domain of GABA(B2) is activated directly by CGP7930, a positive allosteric modulator of the GABA(B) receptor. J Biol Chem 279: 29085–29091.

Carai MA, Colombo G, Froestl W, Gessa GL (2004). In vivo effectiveness of CGP7930, a positive allosteric modulator of the GABAB receptor. Eur J Pharmacol 504: 213–216.

Christopoulos A (2002). Allosteric binding sites on cell-surface receptors: novel targets for drug discovery. Nat. Rev. Drug Discov. 1: 198–210.

Ciambrone GJ, Liu VF, Lin DC, McGuinness RP, Leung GK, Pitchford S (2004). Cellular dielectric spectroscopy: a powerful new approach to label-free cellular analysis. J Biomol Screen 9: 467–480.

Gjoni T, Urwyler S (2008). Receptor activation involving positive allosteric modulation, unlike full agonism, does not result in GABAB receptor desensitization. Neuropharmacology 55: 1293–1299.

Guery S, Floersheim P, Kaupmann K, Froestl W (2007). Syntheses and optimization of new GS39783 analogues as positive allosteric modulators of GABA B receptors. Bioorg Med Chem Lett 17: 6206–6211.

Im BH, Rhim H (2012). GABA(B) receptor-mediated ERK1/2 phosphorylation via a direct interaction with Ca(V)1.3 channels. Neurosci Lett 513: 89–94.

Jenkins L, Harries N, Lappin JE, MacKenzie AE, Neetoo-Isseljee Z, Southern C, et al. (2012). Antagonists of GPR35 display high species ortholog selectivity and varying modes of action. J Pharmacol Exp Ther 343: 683–695.

Knoflach F, Mutel V, Jolidon S, Kew JN, Malherbe P, Vieira E, et al. (2001). Positive allosteric modulators of metabotropic glutamate 1 receptor: characterization, mechanism of action, and binding site. Proc Natl Acad Sci USA 98: 13402–13407.

Le Foll B, Wertheim C, Goldberg SR (2007). High reinforcing efficacy of nicotine in non-human primates. PloS one 2: e230.

Lhuillier L, Mombereau C, Cryan JF, Kaupmann K (2007). GABA(B) receptor-positive modulation decreases selective molecular and behavioral effects of cocaine. Neuropsychopharmacology 32: 388–398.

Liechti ME, Markou A (2007b). Interactive effects of the mGlu5 receptor antagonist MPEP and the mGlu2/3 receptor antagonist LY341495 on nicotine self-administration and reward deficits associated with nicotine withdrawal in rats. Eur J Pharmacol 554: 164–174.

Liechti ME, Lhuillier L, Kaupmann K, Markou A (2007a). Metabotropic glutamate 2/3 receptors in the ventral tegmental area and the nucleus accumbens shell are involved in behaviors relating to nicotine dependence. J Neurosci 27: 9077–9085.

Meier SD, Kafitz KW, Rose CR (2008). Developmental profile and mechanisms of GABA-induced calcium signaling in hippocampal astrocytes. Glia 56: 1127–1137.

Mombereau C, Kaupmann K, Froestl W, Sansig G, van der Putten H, Cryan JF (2004). Genetic and pharmacological evidence of a role for GABA(B) receptors in the modulation of anxiety- and antidepressant-like behavior. Neuropsychopharmacology 29: 1050–1062.

Mombereau C, Lhuillier L, Kaupmann K, Cryan JF (2007). GABAB receptor-positive modulation-induced blockade of the rewarding properties of nicotine is associated with a reduction in nucleus accumbens DeltaFosB accumulation. J Pharmacol Exp Ther 321: 172–177.

Neetoo-Isseljee Z, MacKenzie AE, Southern C, Jerman J, McIver EG, Harries N, et al. (2013). High-throughput identification and characterization of novel, species-selective GPR35 agonists. J Pharmacol Exp Ther 344: 568–578.

New DC, An H, Ip NY, Wong YH (2006). GABAB heterodimeric receptors promote Ca^{2+} influx via store-operated channels in rat cortical neurons and transfected Chinese hamster ovary cells. Neuroscience 137: 1347–1358.

Park HW, Jung H, Choi KH, Baik JH, Rhim H (2010). Direct interaction and functional coupling between voltage-gated CaV1.3 Ca^{2+} channel and GABAB receptor subunit 2. FEBS Lett 584: 3317–3322.

Paterson NE, Vlachou S, Guery S, Kaupmann K, Froestl W, Markou A (2008). Positive modulation of GABA(B) receptors decreased nicotine self-administration and counteracted nicotine-induced enhancement of brain reward function in rats. J Pharmacol Exp Ther 326: 306–314.

Pinard A, Seddik R, Bettler B (2010). GABAB receptors: physiological functions and mechanisms of diversity. Adv Pharmacol 58: 231–255.

Richardson NR, Roberts DC (1996). Progressive ratio schedules in drug self-administration studies in rats: a method to evaluate reinforcing efficacy. J Neurosci Methods 66: 1–11.

Tu H, Rondard P, Xu C, Bertaso F, Cao F, Zhang X, et al. (2007). Dominant role of GABAB2 and Gbetagamma for GABAB receptor-mediated-ERK1/2/CREB pathway in cerebellar neurons. Cell Signal 19: 1996–2002.

Urwyler S, Mosbacher J, Lingenhoehl K, Heid J, Hofstetter K, Froestl W, et al. (2001). Positive allosteric modulation of native and recombinant gamma-aminobutyric acid(B) receptors by 2,6-Di-tert-butyl-4-(3-hydroxy-2,2-dimethyl-propyl)-phenol (CGP7930) and its aldehyde analog CGP13501. Mol Pharmacol 60: 963–971.

Urwyler S, Pozza MF, Lingenhoehl K, Mosbacher J, Lampert C, Froestl W, et al. (2003). N, N'-Dicyclopentyl-2-methylsulfanyl-5-nitro-pyrimidine-4,6-diamine (GS39783) and structurally related compounds: novel allosteric enhancers of gamma-aminobutyric acidB receptor function. J Pharmacol Exp Ther 307: 322–330.

Urwyler S, Gjoni T, Koljatic J, Dupuis DS (2005). Mechanisms of allosteric modulation at GABAB receptors by CGP7930 and GS39783: effects on affinities and efficacies of orthosteric ligands with distinct intrinsic properties. Neuropharmacology 48: 343–353.

Vanhoose AM, Emery M, Jimenez L, Winder DG (2002). ERK activation by G-protein-coupled receptors in mouse brain is receptor identity-specific. J Biol Chem 277: 9049–9053.

Vlachou S, Guery S, Froestl W, Banerjee D, Benedict J, Finn MG, et al. Repeated administration of the GABA(B) receptor positive modulator BHF177 decreased nicotine self-administration, and acute administration decreased cue-induced reinstatement of nicotine seeking in rats. Psychopharmacology (Berl).

Supporting Information

Additional Supporting Information may be found online in the supporting information tab for this article:

Figure S1. Time course of endogenous $ERK_{1/2}$ phosphorylation after addition of 100 μmol/L of GABA in CHO_{RGBR} and HEK_{HGBR}.
Figure S2. Sequence alignment of rat and human GB2R subunits. Mismatch between amino acids sequences are marked in red.
Figure S3. Chemical structures of GS39783 and its analogs, NVP-998 and BHF177.